ARL-TN-1035 • SEP 2020

MIL-PRF-32662: Adhesive, High-Loading Rate, for Structural and Armor Applications—Frequently Asked Questions

by Berend Rinderspacher, Brian Placzankis, William Lum, and Robert Jensen

NOTICES

Disclaimers

The findings in this report are not to be construed as an official Department of the Army position unless so designated by other authorized documents.

Citation of manufacturer's or trade names does not constitute an official endorsement or approval of the use thereof.

Destroy this report when it is no longer needed. Do not return it to the originator.

ARL-TN-1035 ● SEP 2020

MIL-PRF-32662: Adhesive, High-Loading Rate, for Structural and Armor Applications—Frequently Asked Questions

Berend Rinderspacher, Brian Placzankis, William Lum, and Robert Jensen
Weapons and Materials Research Directorate, CCDC Army Research Laboratory

REPORT DOCUMENTATION PAGE

Form Approved
OMB No. 0704-0188

1. REPORT DATE *(DD-MM-YYYY)*	2. REPORT TYPE	3. DATES COVERED (From - To)
September 2020	Technical Note	April 1–September 30, 2020

4. TITLE AND SUBTITLE
MIL-PRF-32662: Adhesive, High-Loading Rate, for Structural and Armor Applications—Frequently Asked Questions

5a. CONTRACT NUMBER

5b. GRANT NUMBER

5c. PROGRAM ELEMENT NUMBER

6. AUTHOR(S)
Berend Rinderspacher, Brian Placzankis, William Lum, and Robert Jensen

5d. PROJECT NUMBER

5e. TASK NUMBER

5f. WORK UNIT NUMBER

7. PERFORMING ORGANIZATION NAME(S) AND ADDRESS(ES)
CCDC Army Research Laboratory
ATTN: FCDD-RLW-MC
Aberdeen Proving Ground, MD 21005-5069

8. PERFORMING ORGANIZATION REPORT NUMBER
ARL-TN-1035

9. SPONSORING/MONITORING AGENCY NAME(S) AND ADDRESS(ES)

10. SPONSOR/MONITOR'S ACRONYM(S)

11. SPONSOR/MONITOR'S REPORT NUMBER(S)

12. DISTRIBUTION/AVAILABILITY STATEMENT
Approved for public release; distribution is unlimited.

13. SUPPLEMENTARY NOTES
Send comments or inquiries to: robert.e.jensen.civ@mail.mil
ORCID(s): Robert Jensen, https://orcid.org/0000-0003-3824-4767; Berend Rinderspacher, https://orcid.org/0000-0003-1333-1653

14. ABSTRACT
This report provides the Frequently Asked Questions (FAQs) and responses as future reference for the users of Military Performance Specification, MIL-PRF-32662 *Adhesive, High-Loading Rate, for Structural and Armor Applications*.

15. SUBJECT TERMS
adhesives, high-loading rate, standardization, federated learning, MIL-PRF-32662

16. SECURITY CLASSIFICATION OF:			17. LIMITATION OF ABSTRACT	18. NUMBER OF PAGES	19a. NAME OF RESPONSIBLE PERSON
a. REPORT	b. ABSTRACT	c. THIS PAGE			Robert E Jensen
Unclassified	Unclassified	Unclassified	UU	33	19b. TELEPHONE NUMBER (Include area code) 240-676-9401

Contents

List of Figures

List of Tables

1. Introduction/Purpose

This report provides Frequently Asked Questions (FAQs) and responses as future reference for the users of Military Performance Specification, MIL-PRF-32662 *Adhesive, High-Loading Rate, for Structural and Armor Applications*,[1] whose purpose is to serve as an anticipatory guidance to discern potential low- and high-ballistic performers with a minimal experimental entry barrier cost.

2. FAQs

2.1 Why the Single-Lap Joint?

ASTM D1002 *Standard Test Method for Apparent Shear Strength of Single-Lap-Joint Adhesively Bonded Metal Specimens by Tension Loading (Metal-To-Metal)*[2] was chosen for the following reasons:

1) ASTM D1002 is a common adhesively bonded joint configuration in academic research.* Single-lap joints with thin adherends can be prepared with minimal assembly tolerance controls, such as using paperclips to maintain bonding pressure, alignment, and overlap length.[3] Additionally, analytical stress distribution modeling of the single-lap joint, bonded with thin adherends, has been a continuous topic of academic interest since the 1930s.[4–9]

2) ASTM D1002 is frequently referenced by adhesive formulators in the technical datasheets (TDSs) for their products. Figure 1 shows a representative example from the TDS for Loctite Hysol EA9309NA epoxy paste adhesive, which has been characterized previously by US Army Combat Capabilities Development Command (CCDC) Army Research Laboratory (ARL).[10]

*Google Scholar (accessed June 29, 2020) cites the thin-adherend single-lap joint ASTM D1002 4090 times versus 153 times for the thick-adherend version ASTM D3937.

Bond Strength Performance

Tensile Lap Shear Strength - tested per ASTM D1002. Adherends are aluminum as referenced and treated with Phosphoric Acid Anodizing (PAA) per ASTM D3933.

	Typical Results			
	7075-T3 Alclad / PAA 3 days @ 77°F/25°C		2024-T3 Alclad / PAA 1 hour @ 180°F/82°C	
Test Temperature, °F/°C	psi	MPa	psi	MPa
-67/-55	4,000	27.6	6700	46.2
77/25	5,000	34.5	6100	42.1
180/82	600	4.1	1300	9.0
77/25 (Hot/Wet) 750 hours @ 160°F/71°C & 85% RH	-	-	5700	39.3

Fig. 1 Excerpt from commercial TDS reporting adhesive bonds strengths determined using ASTM D1002 for guidance[11]

ASTM D1002 is a demonstrated bonded joint configuration that is simple to fabricate and test. Furthermore, ASTM D1002 has an established historical precedence for both academic study and commercial vendor strength reporting.

3) The history and rationale for the correlating single-lap-joint strength and displacement at failure to ballistic damage tolerance requirements are reported in ARL-SR-0371.[12] The difficulties of adhesive bonding for armor applications are described as follows:

- Experimental and modeling challenges: The loading conditions experienced by ground combat vehicles during high-strain-rate/high-stress (ballistic) events are complex.[13–22]
- Variable high-loading-rate environments: Lightweight armor configurations are constantly evolving as new threats are encountered.[23–29]
- Minimal linkages to academia and industry: Little information pertaining to armor configurations in the open literature exists.

The point of this discussion is that actual live-fire ballistic range testing (Fig. 2, left) of adhesively bonded armor assemblies is labor/testing facilities intensive and costly. Yet, following postmortem analysis and analytical/computational modeling of the ballistic response, the failure mechanisms of the adhesive can still remain elusive and often display mixed-mode failure mechanisms.

In contrast, the single-lap joint, per ASTM D1002[2] (Fig. 2, right), is a universally applied adhesive testing configuration that presents ease in experimental accessibility. Qualitative trends emerge by coupling the strength *and* the displacement at failure of the single-lap joint that are adequate in discerning both undesirable and desirable mechanical response in relation to the ballistic damage tolerance of the adhesive. It is statistically unknown if implementing a more

sophisticated experimental technique (hence prohibitive) to derive either truer Mode I tensile or Mode II in-plane shear loading in the adhesive would translate to improved predictions of ballistic damage tolerance.

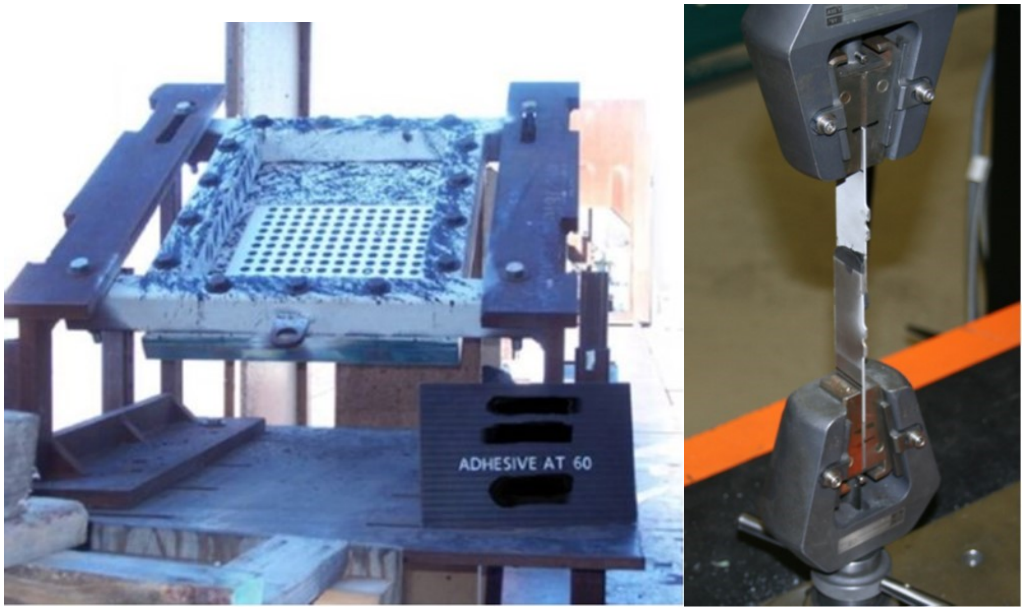

Fig. 2 (Left) Adhesively bonded armor assembly mounted at 60° obliquity to the incoming projectile for live-fire ballistic testing. Note the viewer's perspective is from behind the armor target, which shows the patterning used to measure high-speed 3-D backface deformation via digital image correlation. The armor package is rotated downward to direct fragment ricochets toward the ground. (Right) The single-lap joint presents a simple and universally recognized adhesive testing configuration.

2.2 What About Adherend Deformation in the Single-Lap Joint?

The single-lap joint, with standard ASTM D1002-specified 1.62-mm-thick aluminum (Al) 2024 T3 adherends, is useful in discerning potential ballistic damage tolerant adhesives in part because of the ductility/displacement contribution of the Al 2024 substrate to the overall load displacement curve generated during testing. Figure 3 shows a plot of maximum strength versus displacement at complete failure for a variety of adhesives by the CCDC Army Research Laboratory. Note that if the failure displacement were ignored, it would be impossible to discern favorable Group I performers based only on strength. Some adhesives that have demonstrated improved qualitative ballistic damage tolerance properties have lower strengths than many of the more structurally focused Group II adhesives. Increasing the adherend thickness decreases the displacement at failure of the single-lap joint and increases apparent strength, which will shift and compress the data presented in Fig. 3.[30] Therefore, minimizing the overall joint compliance will make discerning the Group I, II, and III categories more difficult.

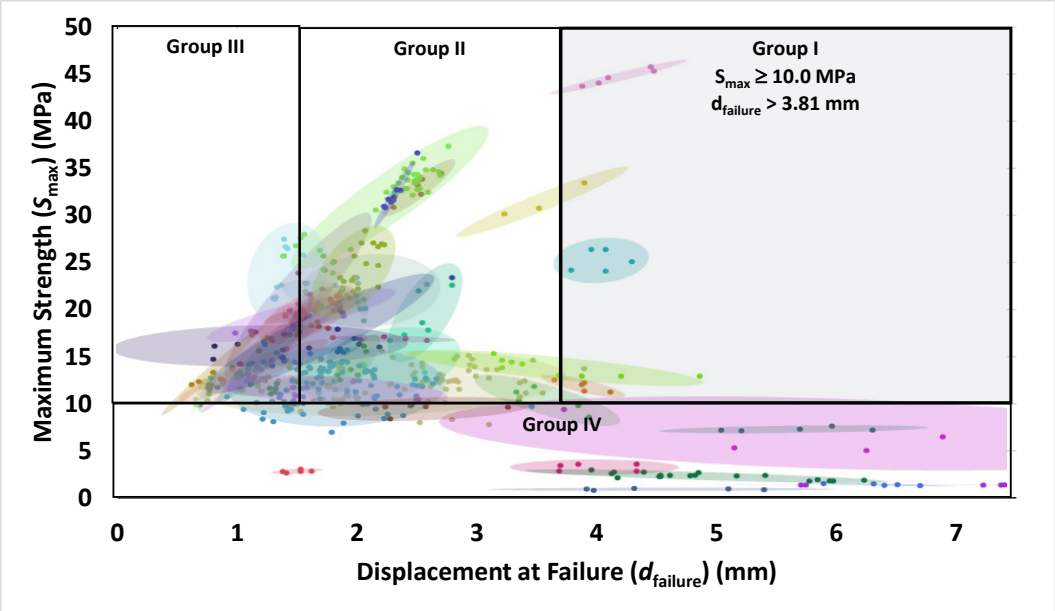

Fig. 3 ARL experimental population of adhesive groups based upon single-lap-joint strength and failure displacement performance at room temperature (dry conditioning). The 90% bivariate normal density ellipses were calculated using JMP Statistical Discovery 14.2.0.[31]

2.3 Can Adhesives Be Classified Using Displacement at Maximum Load?

Figure 4 shows maximum strength plotted versus displacement at maximum load. The data set comprises 573 points and shifts to the left by 0 to 4.53 mm (average 0.34 mm). The Group I outliers are still evident, but the other groups are compressed to varying degrees. Regardless, as the qualifying data for MIL-PRF-32662 is digitally captured, alternative representations are readily available.

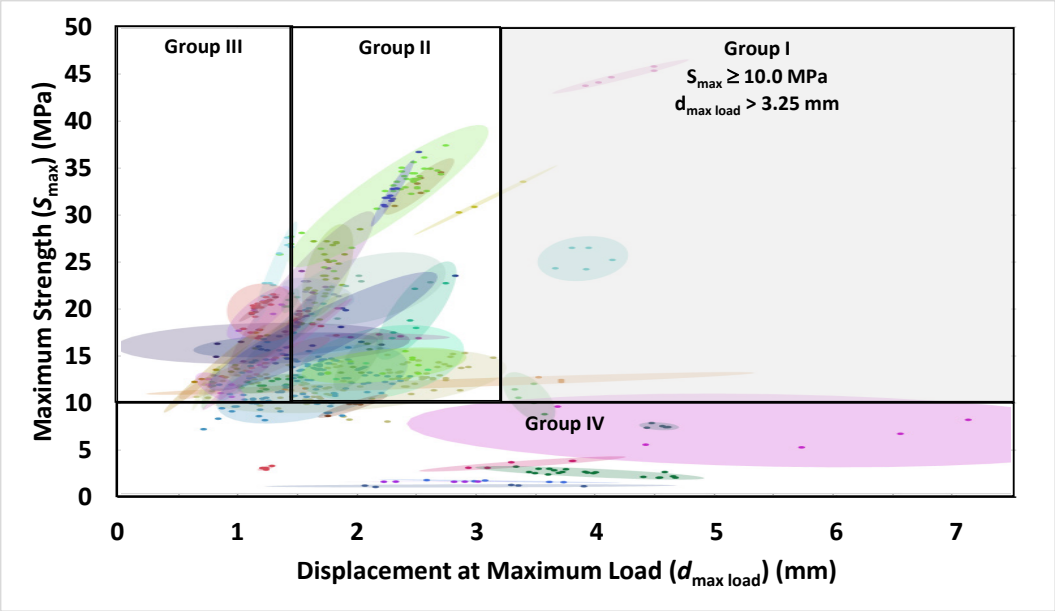

Fig. 4 ARL experimental population of adhesive groups based upon single-lap-joint strength and displacement at maximum load (room temperature, dry conditioning)

2.4 Are there Considerations for Measuring G_{IC} and G_{IIC}?

MIL-PRF-32662 relies on ASTM D1002-based single-lap-joint testing to correlate the holistic response of the bonded joint assembly to ballistic damage tolerance. While the single-lap joint is experimentally simple to process and test, analysis of the adhesive response is difficult due to shear-lag in the overlap region and its resultant mixed-mode loading characteristics. The purpose of MIL-PRF-32662 is to serve as an anticipatory[32] guidance to discern potential low and high ballistic performers with a minimal experimental entry barrier cost. Deriving the precise mechanical properties of the adhesive is not the purpose of MIL-PRF-32662.

While MIL-PRF-32662 does not require rigorous Mode I or Mode II characterization of the adhesive, following the specified test plan does provide double-cantilever-beam (DCB) sample accessibility for determining these values. Post machining of the bonded 300- × 350-mm 2024-T3 Al plates for Tier III crack extension testing will yield 10 individual samples, as shown in Fig. 5, of which only half are required. The five required samples are used for determining the Mode I tensile strain energy release rate while undergoing stress corrosion cracking (G_{ISCC}) at a constant loading tip displacement, as shown in Fig. 6.

The extra five samples are readily adaptable to variable static and cyclic loading conditions per ASTM D3433[33] and ISO 15114[34] for determining G_{IC} and G_{IIC}, respectively. While not required, these measurements are certainly not discouraged.

Fig. 5 Post machining of the bonded 300- × 350-mm 2024-T3 Al for Tier III crack extension testing will yield 10 individual samples

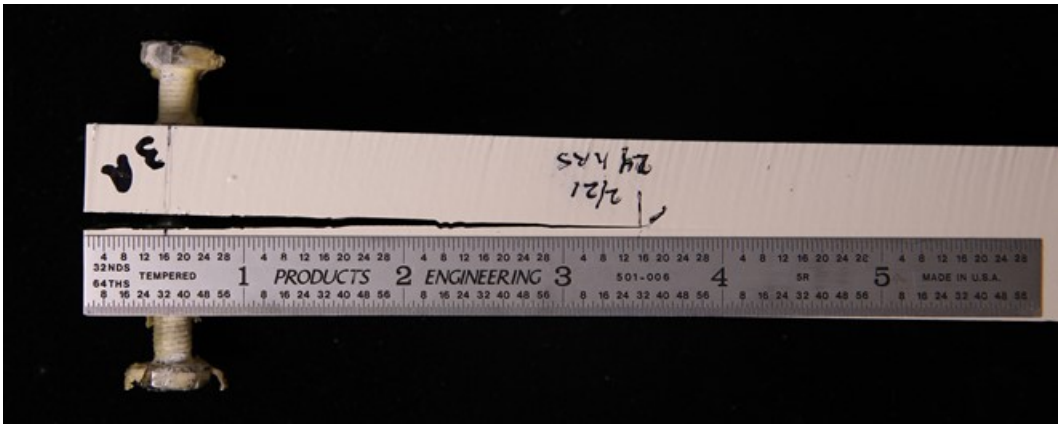

Fig. 6 DCB specimen subjected to constant load tip displacement. This geometry configuration is readily amendable to varied static and cyclic loading conditions needed to rigorously determine the fracture toughness of the adhesive.

2.5 Why Is Displacement at Failure Used and How is it Defined?

A ballistic event near the protection limit of the bonded armor assembly will without exception result in 100% failure of the adhesive. Any linear or nonlinear strain energy absorption mechanism that the adhesive can sustain to this inevitable 100% load drop capacity is potentially beneficial in localizing the damage area.

Figure 7 shows the single-lap-joint load versus displacement response for a polyurethane thermosetting adhesive that meets Group I performance at room temperature. The displacements for yielding,[35] maximum load, and complete failure are 0.82, 1.40, and 4.16 mm, respectively. This sample failed by reaching a failure displacement that exceeded the yield and maximum loading points by 407% and 197%, respectively. Bonded armor packages undergo complete failure in the adhesive, thus the entire loading response of the single-lap joint is considered.

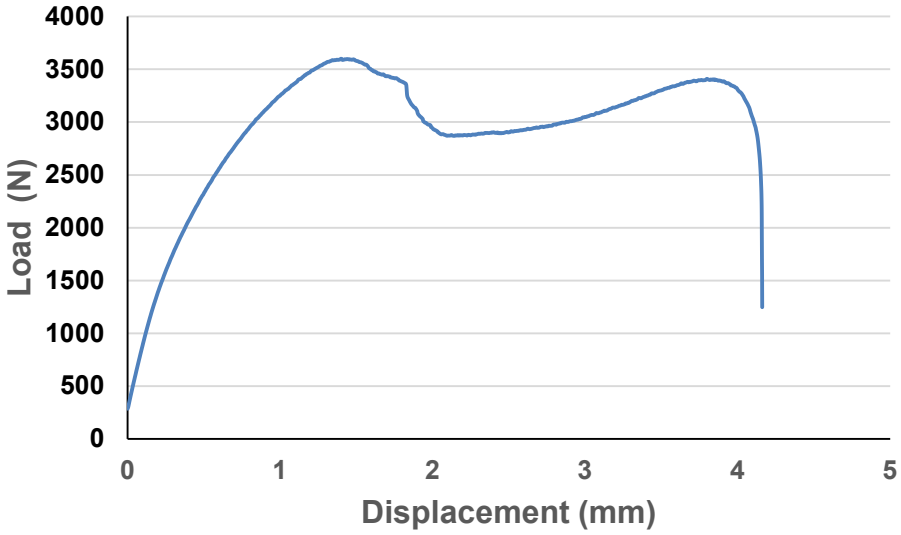

Fig. 7 Single-lap-joint load vs. displacement response for a polyurethane thermosetting adhesive that meets Group I performance at room temperature

Displacement at failure is defined as the displacement where the samples carry no load and the adherends have visibly separated. The incorporation of observing the visible separation of the adherends is to verify failure in the event that data collection frequency of the loading frame does not capture the load cell returning to zero.

2.6 Is Crosshead Displacement Accurate Enough?

The inaccuracy of using direct crosshead displacement measurements for determining strain (ε) under certain conditions is known. Strain is defined as the change in length under deformation loading of a sample in relation to its original length. A material's stiffness modulus (E) is calculated by taking the initial linear slope from a plot of stress (σ, force per unit cross-sectional area) versus strain.

Crosshead displacement on universal testing machines is generally very accurate, as it is the loading frame and load string compliance that introduces error when

precise strain measurements are needed. Errors in strain calculations will be more pronounced when taken at low crosshead displacements.

Figure 8 shows a typical dogbone sample used for measuring tensile properties. The sample has been patterned with a marking pen to obtain high-resolution strain measurements using digital image correlation (DIC), which eliminates strain contributions due to the loading frame and load string compliance.

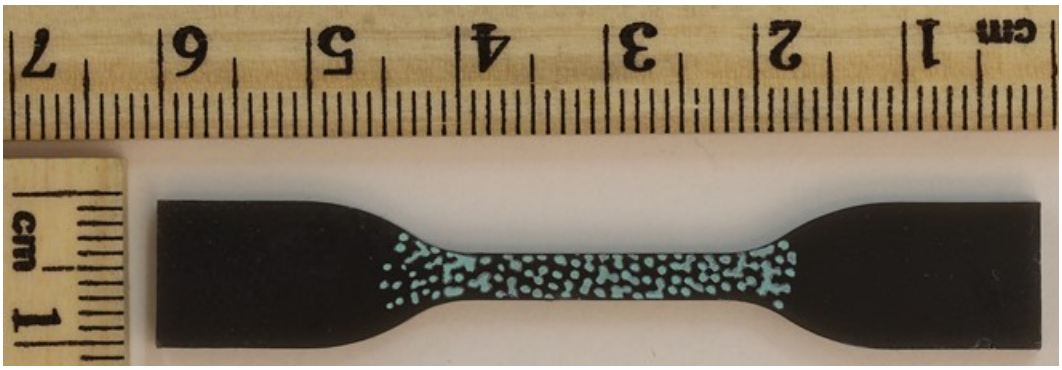

Fig. 8 Tensile dogbone sample of a bulk thermosetting methacrylate adhesive to be tested per ASTM D638-14[36]

Figure 9 shows the resultant stress versus strain curves for this adhesive with strain determined using both DIC and taken directly from the crosshead displacement. The contribution of the load frame and load string compliance to the "apparent" decrease in the stiffness of the sample is obvious when using crosshead displacement.

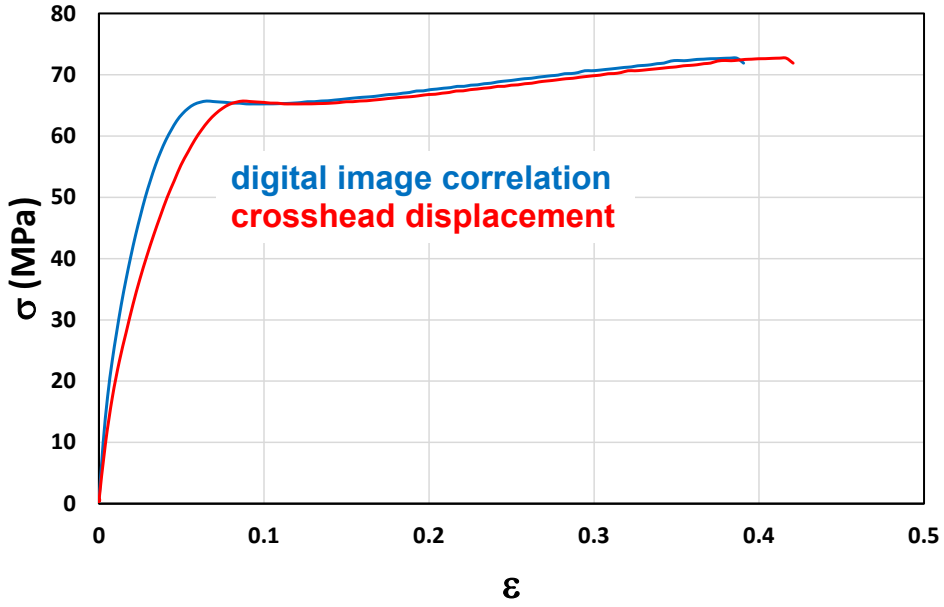

Fig. 9 Room-temperature tensile stress (σ) vs. strain (ε) testing of a thermosetting methacrylate adhesive showing strain determined from both DIC and crosshead displacement

Figure 10 shows the relative percentage error between the crosshead displacement and strain measurements versus crosshead displacement. The error is significant at low displacements, but decreases substantially at extensions greater than 4 mm. Using the data from Fig. 9, the modulus decreases by 60% from 2.19 to 0.88 GPa (at 2.5% strain) from the DIC to crosshead displacement measurements, respectively. At high displacement, the failure strain increases by only 7.5% from 38.7% to 41.6% from the DIC to crosshead displacement measurements, respectively.

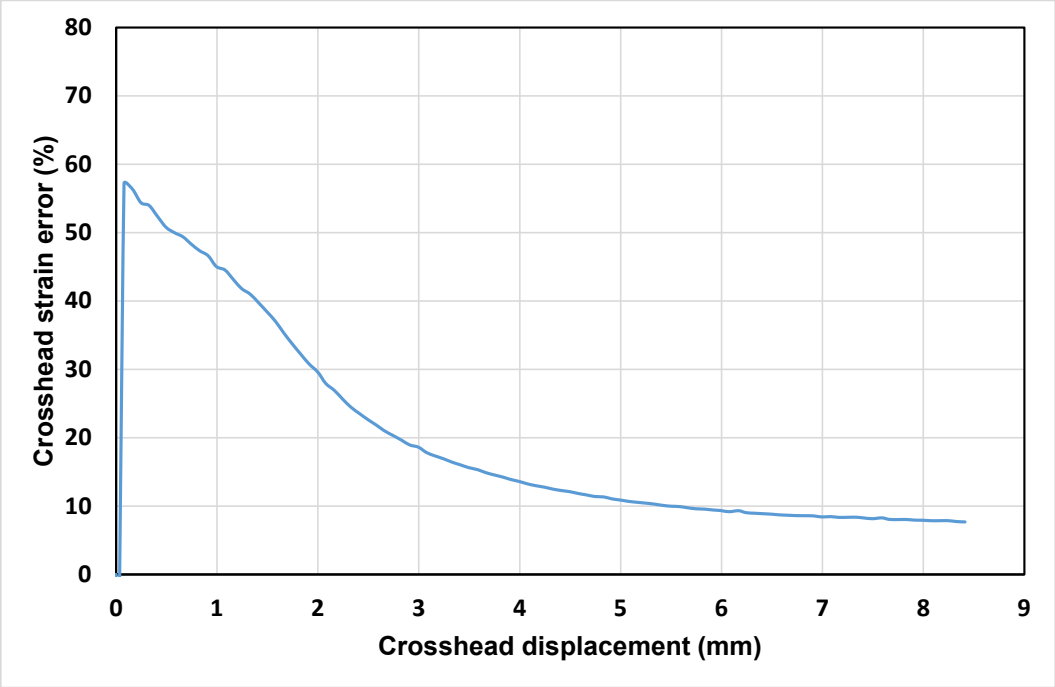

Fig. 10 Relative percentage error between the crosshead displacement and strain measurements vs. crosshead displacement

For the single-lap joint, measuring strain to determine modulus at low crosshead displacements is not relevant. However, error in the displacement measurements of single-lap joints can occur by neglecting to correct for unloaded free play in the load string during the initial displacement, as shown in Fig. 11.

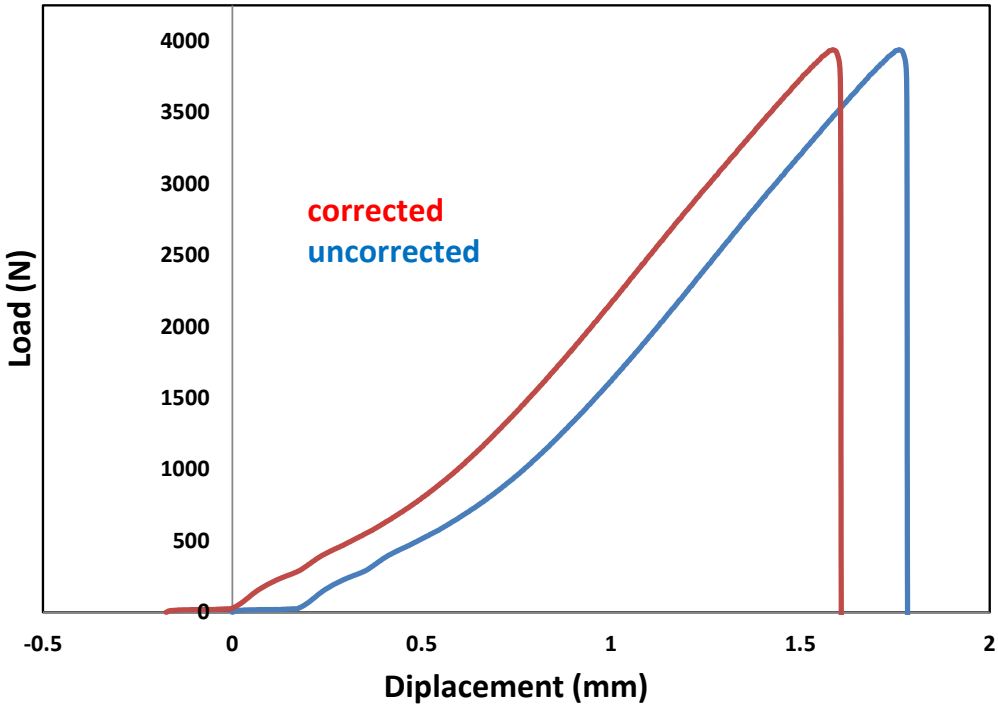

Fig. 11 Single-lap-joint mechanical response showing corrected and uncorrected load string free play during the initial unloaded displacement

The load string shown in Fig. 11 is typical for measuring single-lap-joint mechanical response. ARL has obtained similar single-lap-joint results for the same adhesive tested independently by external organizations. If a similar load string is used then the compliance contributions should be relatively equivalent. The additional use of an extensometer adds more effort to the measurement where the Group I outliers are already apparent from the less-complicated direct crosshead displacement measurements.

Statistical analysis of 1,200 samples shows minimal disparity between load frames for single-lap-joint measurements.[32] This work used a combination of three loading frames and five load cells, with each configuration having its own unique calibration factor. Principal component analysis (PCA) showed that the mechanical response of the single-lap joint is dominated by the adhesive type, surface pretreatment, adherend thickness, and bondline thickness. No significant correlation was found between either strength or displacement to failure with the load string combination.

Multiple linear regression analysis, including application of the Boruta algorithm method based on Random Forests, also confirmed the negligible influence of the loading frame/load cell combinations.*

This data is available in the public domain at https://materialsdata.nist.gov/handle/11256/594.

2.7 Why Is Low Temperature Testing Not Considered?

Table 1 shows single-lap-joint strengths for various adhesives measured by ARL at room, low, and elevated temperatures. The strengths at low temperature either remain within statistical error of the room-temperature values or increase. In comparison, some strength values measured at elevated temperature decrease by statistically significant amounts.

Table 1 Single-lap-joint strengths for various adhesives measured by ARL at room, low,[37] and elevated[38] temperatures

Adhesive	Strength (MPa) RT	Strength (MPa) –51 °C	Strength (MPa) 60 °C
Film epoxy	27.6 ± 1.4	28.3 ± 1.9	23.6 ± 1.1
Paste epoxy	23.3 ± 3.0	20.0 ± 2.2	2.8 ± 0.6
Methacrylate	10.7 ± 0.9	28.3 ± 1.0	5.2 ± 0.3
Thermoplastic polyurethane	9.8 ± 1.0	…	0.27 ± 0.03
Thermoplastic polyurethane	7.5 ± 0.4	17.2 ± 1.3	0.26 ± 0.05
Thermosetting polyurethane	11.7 ± 0.4	24.2 ± 1.2	6.6 ± 0.3
Silicone	2.3 ± 1.0	2.0 ± 0.2	…
Silicone	2.8 ± 0.4	4.0 ± 0.3	2.6 ± 0.2

From an experimentalist's perspective, cooling a load frame to –51 °C is much more difficult than heating to 60 °C. At 60 °C, the thermal losses of the load string are easily compensated by the power output of the oven chamber. In contrast, at –51 °C, a liquid nitrogen cooling jacket and auxiliary chiller are pushed nearly to the limit by the thermal losses of the load string. An experimentalist's estimate is that the level of difficulty in obtaining low temperature test results increases by a factor of 3 in comparison to measuring elevated-temperature response.

*Multiple linear regression was performed by the Data Science Research Group at Worcester Polytechnic Institute, supported by US Army, ACC-APG- RTP, Cooperative Agreement W911NF-19-2-0112 in partnership with ARL.

2.8 Would Low-Temperature Characterization Correlate to High-Strain-Rate Responses?

Interpreting high-strain-rate adhesive failure mechanisms in bonded armor assemblies is difficult and subjective. The mode of failure in the adhesive often changes between room- and low-temperature testing, with similar changes sometimes apparent at ballistic strain rates. However, the adhesive failure mechanisms in the bonded armor assemblies are also certainly partially driven by complex mixed loading conditions as well as the failure mechanisms of the bonded substrates.

The intricate challenges in correlating low-temperature performance to both static and dynamic failure mechanisms are mirrored extensively in academic peer reviewed literature.[39–55] As previously stated, the purpose of this specification is to serve as an anticipatory guidance to discern potential low- and high-ballistic performers with a minimal experimental entry barrier cost. Low-temperature testing, without a clear correlation path toward ballistic performance, adds a significant experimental testing burden where it is reasonably safe to assume that the static loading capacity of the adhesive will remain acceptable.

2.9 MIL-PRF-32662 Does Not Currently Require Low-Temperature Testing. Are there Conditions Where It Would Be Considered?

As data is acquired under operating conditions in the field, federated learning techniques adapted from constrained edge computing will be able to use this data on an ongoing basis to provide continuously improving insights into adhesive performance.[56] These same techniques will be able to utilize more experimentally taxing characterization techniques if and when they become available. Just as current good manufacturing practices are important to providing safe, cost-effective, and performant products (e.g., in the pharma industry[57]) the dynamic inclusion of the entire knowledge base at a given point in time is both critical and informative for specification qualification.

2.10 Why Are the Processing Descriptions So Vague?

Section 4.5.4.6 *Application life* of MIL-PRF-32662 intentionally encompasses a broad range of possible interpretations. Adhesives are available in film, 1-component paste, 2-component paste, solvent cast, hot melt, pressure sensitive, and spray forms. The number of processing variations available for bonded ground vehicle armor assemblies are beyond the scope of this performance specification. However, flat-panel bonded armors for ground vehicles can present a significant

challenge due to their relatively large surface areas and often complex multiple step assembly sequences. For example, Fig. 12 shows the manual application of a 2-component paste adhesive to an approximately 1.5- × 1.5-m section of rolled homogeneous armor (RHA) steel.

Fig. 12 Application of a 2-component paste adhesive to a section of RHA steel. Note: The RHA steel was grit blasted and pretreated with a commercially available non-chromate wash-primer prior to bonding per TT-C-490G.[58]

Likewise, Sections 3.5.1.1 *Viscosity*, 3.5.1.2 *Pot life/Open time*, 3.5.1.3 *Sag and Bridging,* 3.5.1.4 *Curing pressure*, and 3.5.1.5 *Curing time and temperature* are also deliberately written to encompass a broad range of possible processing conditions. However, these minimally constrained adhesive and processing requirements must converge to successfully meet Section 4.5.4.4 *Tier III: Crack extension test* requirements, which calls for bonding two 300- × 350-mm 2024-T3 Al plates. These plate dimensions are adequate to screen processing suitability for larger bonded armor assemblies. Passing Section 4.5.4.4 *Tier III: Crack extension test* requirements necessitates high quality with respect to the absence of voiding, consistent bondline thickness, and full adhesive cure, which is the embodiment of the product characteristics called-out in MIL-PRF-32662. An example of processing a bonded set of *Tier III: Crack extension test* plates is shown in Figs. 13–16.

Fig. 13 Representative example of the manual application of a 1-component paste adhesive to 300- × 350-mm 2024-T3 Al plates for required for the Tier III: Crack extension test

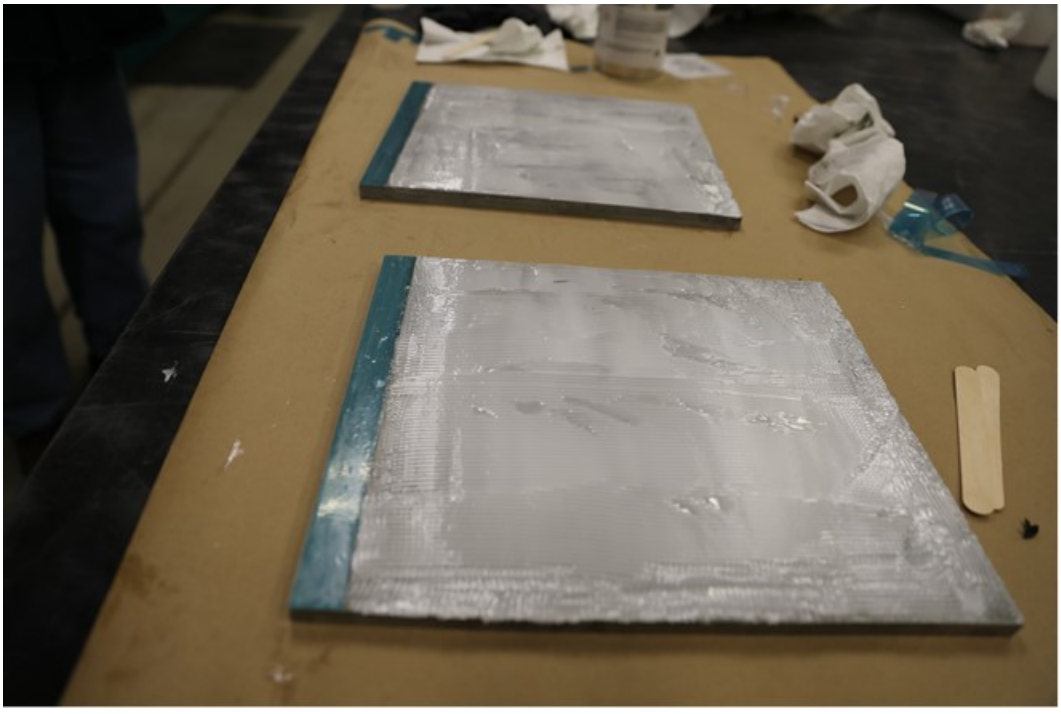

Fig. 14 Representative example of the manual spreading of a 1-component paste adhesive

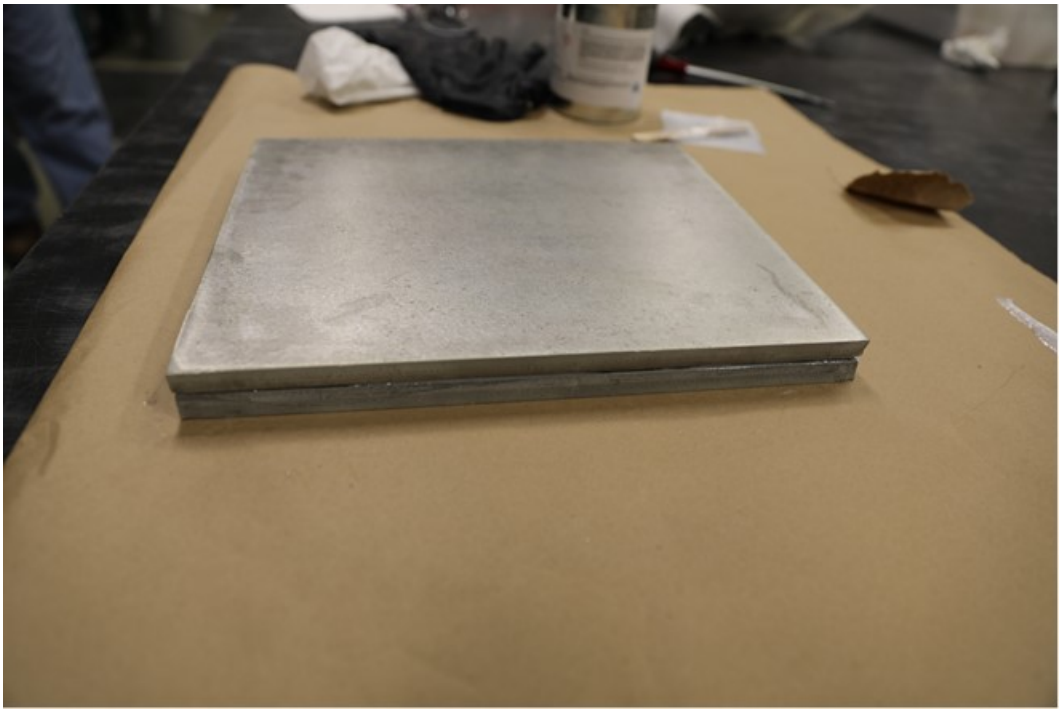

Fig. 15 Sandwiching the two 300- × 350-mm 2024-T3 Al plates together prior to curing the adhesive

Fig. 16 Curing the two 300- × 350-mm 2024-T3 Al plates together under vacuum pressure at elevated temperature

2.11 Why Is the Test Method for Sag and Bridging Not Specified?

Inadequate thixotropic static flow characteristics will result in excessive bondline voiding and/or thickness inconsistencies, which will reduce the probability of passing the Section 4.5.4.4 *Tier III: Crack extension test* requirements.

2.12 Can Examples of Conditioning in Hot Water or at Elevated Temperature Be Shown?

Figure 17 shows an experimental setup for meeting MIL-PRF-32662 4.5.4.2 *Tier II: Single-lap-joint hot/wet strength retention test* requirements. The tensile shear test shall be in accordance with Section 4.5.4.1 after submersion of lap-joint specimens in a water immersion tank for 14 days at a constant temperature of 63 ± 3 °C (145 ± 5 °F). At the completion of the conditioning, specimens will be pat-dried and tested no later than 30 min after being removed from the water immersion tank.

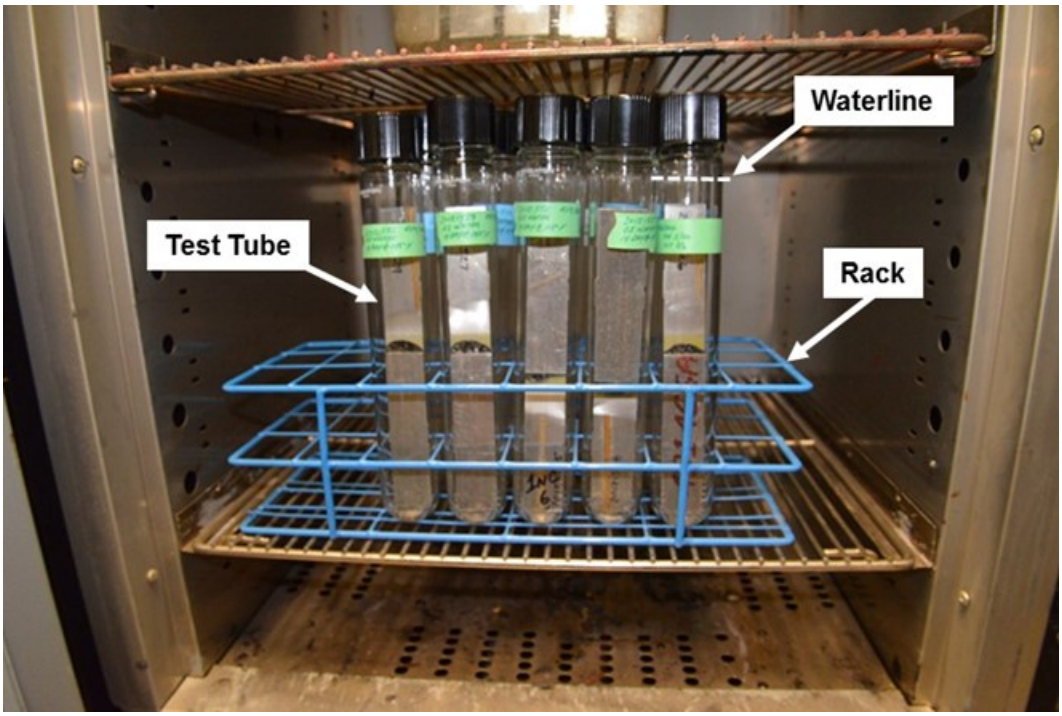

Fig. 17 Alternate elevated temperature/water immersion conditioning test for lap-joint test specimens using the test tubes and convection oven method. From ARL-SR-0356.[59]

Section 4.5.4.3 *Tier II – Part 2: Single-lap-joint elevated temperature strength retention test*, requires for the shear strength measurement to be taken at 71 °C ± 3 °C. A common practice would be to condition the test samples for 45 min, while loaded in the testing grips, in the test frame oven, as shown in Fig. 18.

The document formatting for this performance specification describes the sample conditioning and testing procedures in different sections. It is implied that the elevated temperature conditioning would occur in the test grips while mounted in the loading frame.

Fig. 18 Samples undergoing elevated temperature testing at 71 °C ± 3 °C (160 °C ± 5 °F), with the chamber door opened (left) and closed (right). Thermocouple (TC) is also shown. From ARL-SR-0356.[59]

2.13 Are Groups II, III, and IV Relevant?

Group I represents a challenging performance region, with potentially enhanced ballistic damage tolerance in some bonded armor configurations, which is not easily obtainable by current commercial products. Group II, III, and IV adhesives also have utility in other armor configurations. This standard provides a test methodology to rapidly analyze Group II, III, and IV adhesives for potential service life issues.

Figure 19 shows an adhesive bonding failure at a ceramic–composite interface that presented issues after several years of field service. ARL was able to replicate the service failure within 24 h of Tier II hot/wet testing, per Section 4.5.4.2. This specification provides a rapid screening approach to minimize future service life issues where a Group II, III, or IV adhesive is selected for bonding in an armor configuration.

Fig. 19 Adhesive failure at the ceramic–composite interface due to ambient environmental exposure

3. Conclusion

This report provides FAQs and responses as future reference for the users of MIL-PRF-32662 *Adhesive, High-Loading Rate, for Structural and Armor Applications*,[1] whose purpose is to serve as an anticipatory guidance to discern potential low- and high-ballistic performers with a minimal experimental entry barrier cost. The approaches taken in MIL-PRF-32662 are non-traditional from standard practice, therefore end users are encouraged to contact the authors for discussion and suggestions.

4. References

1. MIL-PRF-32662. Adhesive, high-loading rate, for structural and armor applications. Aberdeen Proving Ground (MD): CCDC Army Research Laboratory (US); 2020 Aug 20.

2. ASTM D1002. Standard test method for apparent shear strength of single-lap-joint adhesively bonded metal specimens by tension loading (metal-to-metal). West Conshohocken (PA): ASTM International; 2019. https://www.astm.org/Standards/D1002.htm.

3. Shahzad MF, Mughal MP, Iqbal HMS, Mufti NA, Saleem MQ. Polybenzimidazole adhesive bonded aluminum-2024 joints for structural applications. International Journal of Adhesion and Adhesives. 2019;95:1–6. https://doi.org/10.1016/j.ijadhadh.2019.102433.

4. Volkersen O. Die niektraftverteilung in zugbeanspruchten nietverbindungen mit konstanten laschenquerschnitten. Luftfahrtforschung. 1938;15:41–47.

5. da Silva LFM, das Neves PJC, Adams RD, Spelt JK. Analytical models of adhesively bonded joints – Part I: Literature survey. International Journal of Adhesion and Adhesives. 2009;29:319–330.

6. da Silva LFM, das Neves PJC, Adams RD, Wang A, Spelt JK. Analytical models of adhesively bonded joints – part II: comparative study. International Journal of Adhesion and Adhesives. 2009;29:331–341. doi:10.1016/j.ijadhadh.2008.06.007

7. Taib AA, Boukhili R, Achiou S, Gordon S, Boukehili H. Bonded joints with composite adherends. part I. effect of specimen configuration, adhesive thickness, spew fillet and adherend stiffness on fracture. International Journal of Adhesion and Adhesives. 2006;(26):226–336. doi:10.1016/j.ijadhadh.2005.03.015

8. Weibgraeber P, Felger J, l'Armee AT, Becker W. Crack initiation in single lap joints: effects of geometrical and material properties. International Journal of Fracture. 2015;192:155–166. doi: 10.1007/s10704-015-9992-6

9. Ramalho LDC, Campilho RDSG, Belinha J. Single lap joint strength prediction using the radial point interpolation method and the critical longitudinal strain criterion. Engineering Analysis with Boundary Elements. 2020;113: 268–276. doi: 10.1016/j.enganabound.2020.01.010

10. Jensen R, Flanagan D, DeSchepper D, Silton M. Single-lap-joint screening of hysol EA 9309NA epoxy adhesive. Aberdeen Proving Ground (MD): Army Research Laboratory (US); 2017 May. Report No.: ARL-TR-8011.

11. Loctite EA 9309NA AERO epoxy paste adhesive. Technical Process Bulletin. Henkel Corporation Aerospace; 2015 July. https://www.pccomposites.com/wp-content/uploads/2015/07/PCRS9309-QT_TDS.pdf.

12. Jensen R, Flanagan D, DeSchepper D, Pergantis C. Adhesives: test method, group assignment, and categorization guide for high-loading-rate applications – history and rationale. Aberdeen Proving Ground (MD): Army Research Laboratory (US); 2017 Apr. Report No.: ARL-SR-0371.

13. Carton EP, Johnsen BB, Rahbek DB, Broos H, Snippe A. Round robin using the depth of penetration test method on an armour grade alumina. Defence Technology. 2019;15:829–836. doi: 10.1016/j.dt.2019.07.014.

14. Yao RX, Su F, Mao RH. Influence of interfacial bonding conditions on the anti-penetration performance of ceramic/metal composite targets. Materials Science and Engineering. 2019;15:833–844. doi: 10.1007/s10999-019-09445-1.

15. Tepeduzu B, Karakuzu R. Ballistic performance of ceramic/composite structures. Ceramics International. 2019;24:259–275. doi: 10.1016/j.ceramint.2018.10.042.

16. Madhu V, Ramanjaneyulua K, Bhat TB, Gupta NK. An experimental study of penetration resistance of ceramic armour subjected to projectile impact. International Journal of Impact Engineering. 2005;45:1651–1660.

17. Gupta N, Prasad VVB, Madhu V, Basu B. Ballistic studies on TiB2-Ti functionally graded armor ceramics. Defence Science Journal. 2012;62:382–389.

18. Deka LJ, Bartus SD, Vaidya U.K. Multi-site impact response of S2-glass/epoxy composite laminates. Composites Science and Technology. 2009; 69:725–735.

19. Tasdemirci A, Hall IW. Numerical and experimental studies of damage generation in multi-layer composite materials at high strain rates. International Journal of Impact Engineering. 2007;34:189–204.

20. Bartus SD, Vaidy UK. A review: impact damage of composite materials. Journal of Advanced Materials. 2007;39:3–21.

21. Resnyansky AD The impact response of composite materials involved in helicopter vulnerability assessment: literature review – part 1. Edinburgh (South Australia): Defence Science and Technology Organisation; 2006. DSTO Report No.: DSTO-TR-1842 Part 1.

22. Resnyansky AD. The impact response of composite materials involved in helicopter vulnerability assessment: literature review – part 2. Edinburgh (South Australia): Defence Science and Technology Organisation; 2006. Report No.: DSTO-TR-1842 Part 2.

23. Deka LJ, Bartus SD, Vaidya UK. Multi-site impact response of s2-glass/epoxy composite laminates. Composites Science and Technology. 2009;69:725–735.

24. Deka LJ, Bartus SD, Vaidya UK. Damage evolution and energy absorption of e-glass/polypropylene laminates subjected to ballistic impact. Journal of Materials Science. 2008;43(13):4399–4410.

25. Bartus SD. A review: impact damage of composite materials. Journal of Advanced Materials. 2007;39(3):3–21.

26. Bogetti TA, Hoppel CPR, Harik VM, Newill JF, Burns BP. Predicting the nonlinear response and failure of composite laminates: Correlation with experimental results. Composites Science and Technology. 2004;64:477–485.

27. STANAG 4569. Procedures for evaluating the protection level of logistic and light armoured vehicles. Brussels (Belgium): North Atlantic Treaty Organization; 2012.

28. Pratomo AN, Santosa SP, Gunawan L, Putra IS. Countermeasures design and analysis for occupant survivability of an armored vehicle subjected to blast load. Journal of Mechanical Science and Technology. 2020;34:1893–1899. doi: 10.1007/s12206-020-0411-1

29. Purchase Description Transparent Armor. Warren (MI): US Army Tank-Automotive and Armaments Command; 26 Apr 2010. Metric ATPD 2352R.

30. Jensen RE, DeSchepper DC, Flanagan DP. Multivariate analysis of high through-put adhesively bonded single lap joints. International Journal of Adhesion and Adhesives. 2019;89:1–10. https://doi.org/10.1016/j.ijadhadh.2018.11.004.

31. SAS web site. Cary (NC): SAS Institute Inc.; 2020 [accessed 2020]. https://www.sas.com/en_us/home.html.

32. Egyedi TM, Sherif MH. Standards dynamics through an innovation lens: next-generation Ethernet networks. IEEE Communications Magazine. 2010;48:166–171. doi: 10.1109/MCOM.2010.5594692.

33. ASTM standard D3433-99. Standard test method for fracture strength in cleavage of adhesives in bonded metal joint. West Conshohocken (PA): ASTM International; 2020.

34. ISO 15114:2014(E). Fibre-reinforced plastic composites — determination of the mode II fracture resistance for unidirectionally reinforced materials using the calibrated end-loaded split (C-ELS) test and an effective crack length approach. Geneva (Switzerland): International Organization for Standardization; 2014.

35. Christensen RM. Observations on the definition of yield stress. Acta Mechanica. 2008;196:239–244. doi: 10.1007/s00707-007-0478-0.

36. ASTM standard D638-14. Standard test method for tensile properties of plastics. West Conshohocken (PA): ASTM International; 2014.

37. MIL-STD-810G. Environmental engineering considerations and laboratory tests, 502.5, low temperature. Aberdeen Proving Ground (MD): Army Test and Evaluation Command; 2008 Oct 31.

38. MIL-STD-810G. Environmental engineering considerations and laboratory tests, 501.5, high temperature. Aberdeen Proving Ground (MD): Army Test and Evaluation Command; 2008 Oct 31.

39. Jia Z, Yuan G, Feng X, Zou Y, Yu J. Shear properties of polyurethane ductile adhesive at low temperatures under high strain rate conditions. Composites Part B. 2019;156:292–302. doi: 10.1016/j.compositesb.2018.08.060.

40. Machado JJM, Marques EAS, Campilho RDSG, da Silva LFM. Mode II fracture toughness of CFRP as a function of temperature and strain rate. Composites Part B. 2017;114:311–318. doi: 10.1016/j.compositesb.2017.02.013.

41. Jia Z, Hui D, Yuan G, Lair J, Lau KT, Xu F. Mechanical properties of an epoxy-based adhesive under high strain rate loadings at low temperature environment. Composites Part B. 2016;105:132–137. doi: 10.1016/j.compositesb.2016.08.034.

42. Jia Z, Yuan G, Ma HL, Hui D, Lau KT, Xu F. Tensile properties of a polymer-based adhesive at low temperature with different strain rates. Composites Part B. 2016;87:227–232. doi: 10.1016/j.compositesb.2015.10.013.

43. Ferrier E, Rabinovitch O, Michel L. Mechanical behavior of concrete–resin/adhesive–FRP structural assemblies under low and high temperatures. Construction and Building Materials. 2016;127:1017–1028. doi: 10.1016/j.conbuildmat.2015.12.127.

44. Melcher RJ, Johnson WS. Mode I fracture toughness of an adhesively bonded composite–composite joint in a cryogenic environment. Composites Science and Technology. 2007;67:501–506. doi: 10.1016/j.compscitech.2006.08.026.

45. Araújo HAM, Machado JJM, Marques EAS, da Silva LFM. Dynamic behaviour of composite adhesive joints for the automotive industry. Composite Structures. 2017;171:549–561. doi: 10.1016/j.compstruct.2017.03.071.

46. Avendaño R, Carbas RJC, Marques EAS, da Silva LFM, Fernandes AA. Effect of temperature and strain rate on single lap joints with dissimilar lightweight adherends bonded with an acrylic adhesive. Composite Structures. 2016;152:34–44. doi: 10.1016/j.compstruct.2016.05.034.

47. Pana L, Zhang A, Zheng Z, Duan L, Zhang L, Shi Y, Tao J. Enhancing interfacial strength between AA5083 and cryogenic adhesive via anodic oxidation and silanization. International Journal of Adhesion and Adhesives. 2018;84:317–324. doi: 10.1016/j.ijadhadh.2018.04.006.

48. LeBono J, Barton L, Birkett M. Low temperature tensile lap-shear testing of adhesively bonded polyethylene pipe. International Journal of Adhesion and Adhesives. 2017;74:57–63. doi: 10.1016/j.ijadhadh.2016.12.003.

49. Hu P, Han X, Li WD, Li L, Shao Q. Research on the static strength performance of adhesive single lap joints subjected to extreme temperature environment for automotive industry. International Journal of Adhesion and Adhesives. 2013;41:119–126. doi: 10.1016/j.ijadhadh.2012.10.010.

50. Grant LDR, Adams RD, da Silva LFM. Effect of the temperature on the strength of adhesively bonded single lap and T joints for the automotive industry. International Journal of Adhesion and Adhesives. 2009;29:535–542. doi: 10.1016/j.ijadhadh.2009.01.002.

51. da Silva LFM, Adams RD. Joint strength predictions for adhesive joints to be used over a wide temperature range. International Journal of Adhesion and Adhesives. 2007;27:362–379. doi: 10.1016/j.ijadhadh.2006.09.007

52. da Silva LFM, Adams RD. Adhesive joints at high and low temperatures using similar and dissimilar adherends and dual adhesives. International Journal of Adhesion and Adhesives. 2007;27:216–226. doi: 10.1016/j.ijadhadh.2006.04.002.

53. Zgoul M, Crocombe AD. Numerical modelling of lap joints bonded with a rate-dependent adhesive. International Journal of Adhesion and Adhesives. 2004;24:355–356.

54. Machado JJM, Nunes PDP, Marques EAS, da Silva LFM. Adhesive joints using aluminium and CFRP substrates tested at low and high temperatures under quasi-static and impact conditions for the automotive industry. Composites Part B. 2019;158:102–116. doi: 10.1016/j.compositesb.2018.09.067.

55. Anes V, Pedro R, Henriques E, Freitas M, Reis L. Bonded joints of dissimilar adherends at very low temperatures – an adhesive selection approach. Theoretical and Applied Fracture Mechanics. 2016;85:99–112. doi: 10.1016/j.tafmec.2016.08.012.

56. McMahan B, Ramage D. Federated learning: collaborative machine learning without centralized training data. Google AI Blog; 2017 Apr 6 [accessed 2020]. https://ai.googleblog.com/2017/04/federated-learning-collaborative.html.

57. Facts about the current good manufacturing practices (CGMPS). Washington (DC): Food and Drug Administration (US); 2018 June 25 [accessed 2020]. https://www.fda.gov/drugs/pharmaceutical-quality-resources/facts-about-current-good-manufacturing-practices-cgmps.

58. TT-C-490G. Chemical conversion coatings and pretreatments for metallic substrates (base for organic coatings). Aberdeen Proving Ground (MD): Army Research Laboratory, Weapons and Materials Research Directorate; 2019 Sep 09.

59. Jensen R, DeSchepper D, Flanagan D, Chaney G, Pergantis C. Adhesives: test method, group assignment, and categorization guide for high-loading-rate applications – preparation and testing of single lap joints (ver. 2.2, unlimited). Aberdeen Proving Ground (MD): Army Research Laboratory (US); 2016 Apr. Report No.: ARL-SR-0356.

List of Symbols, Abbreviations, and Acronyms

3-D	three-dimensional
Al	aluminum
ARL	US Army Research Laboratory
ASTM	ASTM International, formerly known as the American Society for Testing and Materials
DCB	double cantilever beam
$d_{failure}$	displacement at complete failure
DIC	digital image correlation
$d_{max\ load}$	displacement at maximum load
ε	strain
E	modulus
G_{IC}	Mode I critical strain energy release rate
G_{IIC}	Mode II critical strain energy release rate
G_{ISCC}	Mode I tensile strain energy release rate while undergoing stress corrosion cracking
ISO	International Organization for Standardization
PCA	principle component analysis
P_{max}	maximum load
PRF	performance
RHA	rolled homogeneous armor
RT	room temperature
σ	stress
TDS	technical datasheet

1 (PDF)	DEFENSE TECHNICAL INFORMATION CTR DTIC OCA
1 (PDF)	CCDC ARL FCDD RLD DCI TECH LIB
4 (PDF)	CCDC ARL FCDD RLW MC R JENSEN W LUM B PLACZANKIS B RINDERSPACHER